Asymmetries between achromatic increments and decrements: Perceptual scales and discrimination thresholds

Yangyi Shi Department of Psychology, Northeastern University, Boston, MA, USA

Rhea T. Eskew, Jr. Department of Psychology, Northeastern University, Boston, MA, USA

The perceptual response to achromatic incremental (A+) and decremental (A–) visual stimuli is known to be asymmetrical, due most likely to differences between ON and OFF channels. In the current study, we further investigated this asymmetry psychophysically. In Experiment 1, maximum likelihood difference scaling (MLDS) was used to estimate separately observers' perceptual scales for A+ and A–. In Experiment 2, observers performed two spatial alternative forced choice (2SAFC) pedestal discrimination on multiple pedestal contrast levels, using all combinations of A+ and A– pedestals and tests. Both experiments showed the well-known asymmetry. The perceptual scale curves of A+ follow a modified Naka–Rushton equation, whereas those of A– follow a cubic function. Correspondingly, the discrimination thresholds for the A+ pedestal increased monotonically with pedestal contrast, whereas the thresholds of the A– pedestal first increased as the pedestal contrast increased, then decreased as the contrast became higher. We propose a model that links the results of the two experiments, in which the pedestal discrimination threshold is inversely related to the derivative of the perceptual scale curve. Our findings generally agree with Whittle's previous findings (Whittle, 1986, 1992), which also included strong asymmetry between A+ and A–. We suggest that the perception of achromatic balanced incremental and decremental (bipolar) stimuli, such as gratings or flicker, might be dominated by one polarity due to this asymmetry under some conditions.

Introduction

Many studies of achromatic visual perception use gratings or other stimuli that contain balanced regions of both incremental (A+) and decremental (A–) contrast (relative to the mean, time-averaged adapting field). However, it is clear that human perceptions of A+ and A– are qualitatively different in multiple ways (Chichilnisky & Wandell, 1996; Rudd & Zemach, 2004; Rudd & Zemach, 2005; Westheimer, 2007). In the current study, we aimed to investigate these differences in a more comprehensive way, presenting A+ and A– stimuli separately. We compared the perception of achromatic increment (A+) and decrement (A–) square patches by deriving independent perceptual scales for these two polarities and then testing the predictions of forced-choice pedestal discrimination based on these perceptual scales.

In a seminal paper, Whittle (1992) conducted an equal-interval brightness scaling experiment to study the perceptual scales of A+ and A–. The result was asymmetrical around the origin (the background luminance). The perceptual scale curve for the A+ subset of the stimuli was a decelerating function of contrast (Figure 1b), whereas the A– subset looked like a reversed, inverted "S" shape (Figure 1a). Following previous researchers, Whittle referred to the steep portion of the scale near the origin as causing a "crispening" effect (Kaneko, 1964; Takasaki, 1967), or enhanced luminance discrimination near the background luminance.

Discrimination experiments can also be used to study internal representations of magnitude, albeit indirectly. Fechner derived his logarithmic scale of sensory magnitude from Weber's law of discrimination in this fashion (Baird & Noma, 1978; Laming, 1973). Here, we focus on the measurement of pedestal discrimination ("dipper" or threshold-vs.-contrast masking [TvC]) functions (Foley & Legge, 1981; Kwon, Legge, Fang, Cheong, & He, 2009; Nachmias & Kocher, 1970; Nachmias & Sansbury, 1974; Shooner & Mullen, 2022; Solomon, 2009).

Only a few pedestal discrimination studies have directly compared A+ and A– polarities. Whittle (1986) measured two discrimination conditions: incremental tests on both incremental pedestals and decremental pedestals (decremental tests were used instead when decremental pedestal contrast was very low). Whittle found dramatic differences between A+ and A– discrimination, using a complex definition of

Citation: Shi, Y., & Eskew, R. T., Jr. (2024). Asymmetries between achromatic increments and decrements: Perceptual scales and discrimination thresholds. *Journal of Vision*, *24*(4):10, 1–16, https://doi.org/10.1167/jov.24.4.10.

https://doi.org/10.1167/jov.24.4.10 Received September 12, 2023; published April 12, 2024 ISSN 1534-7362

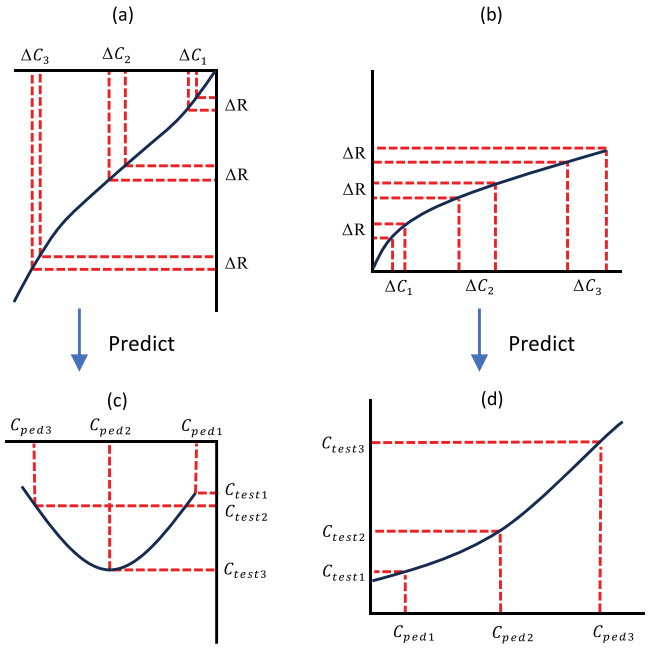

Figure 1. A schematic model of predicting pedestal discrimination threshold using perceptual scale. The left column (a, c) is A–, and the right column (b, d) is A+. The top row is the hypothesized perceptual scale (modified from Whittle, 1992), and the bottom row is the hypothesized prediction of the pedestal discrimination threshold. In (a), the origin is at the top right, representing the adaptation state (or 0 luminance contrast); the horizontal axis is contrast, and the vertical axis is the perceptual scale. Both axes are in negative directions to represent A–. ΔR indicates a fixed-size change in the perceptual scale. As the slope of the scale changes, the required size of contrast change (ΔC) varies. In (c), the origin is again at the top right. The horizontal axis is the pedestal contrast, and the vertical axis is the discrimination threshold contrast at the pedestal level, for decremental tests. Parts (b) and (d) are analogous to (a) and (c) but for A+ (the origin is at bottom left). The steeper the slope of the perceptual scale curve, the smaller the ΔC required to reach the same amount of ΔR change in perceptual scale, so the smaller the pedestal discrimination threshold.

Weber-like contrast (see also Kane & Bertalmio, 2019; Kingdom & Moulden, 1991). Legge and Kersten (1983) studied A+ tests on A+ pedestals and A– tests on A– pedestals, for pedestal strengths ranging from about 0.07× to about 50× threshold. They found only small differences in the shapes of TvCs for the increments and decrements when Michelson contrast was used to characterize tests and pedestals, but reported a larger difference, with less masking for decrements (at high pedestal contrasts), when Weber contrast ($\Delta I/I$) was used. Cole, Stromeyer, and Kronauer (1990) studied pedestal discrimination for equichromatic tests and pedestals (i.e., the tests and pedestals were the same color—yellow—as the background field, so the task was luminance discrimination). Unlike Whittle (1986) and Legge and Kersten (1983), these authors did not find an asymmetry between increments and decrements (their figure 3), even though they used Weber contrast, possibly due to the pedestal contrasts being relatively low.

Figure 1 presents a schematic model, based on Whittle's results, that shows how TvC discrimination functions may be related to internal scales. Figure 1b shows a decelerating perceptual scale for increment stimuli; larger steps in physical contrast (ΔC, horizontal axis) are required to produce the same response (ΔR, vertical axis), producing the accelerating TvC function shown in Figure 1d. This relationship, with the local slope of the perceptual scale determining the shape of the TvC, has been widely exploited for increment tests and for sinusoidal gratings (e.g., Kwon et al., 2009; Shooner & Mullen, 2022). However, Whittle's perceptual scale measurements for A– (schematized in Figure 1a) imply a very different discrimination result, using the same assumptions as for increments (Kane & Bertalmio, 2019; Kingdom & Moulden, 1991). The inverted, reversed "S"-shaped perceptual scale implies the nonmonotonic TvC shown in Figure 1c for decrement tests. An important goal of the current study was to provide a quantitative model that connects scaling results and pedestal discrimination results in A+ and A–.

Our experiment design is similar to those of Whittle (1986), Whittle (1992), but there are several major differences. First, we used maximum likelihood difference scaling (MLDS) to estimate observers' perceptual scales. MLDS, developed by Maloney and Yang (2003), is an efficient method for generating perceptual scales with interval scale properties. Second, Whittle's scaling experiment presented A+ and A– stimuli together on the same screen (in some conditions), whereas our scaling was done for A+ and A– separately. Third, we minimized adaptation to the stimuli by using flashes in the scaling experiment rather than the steadily-viewed tests employed by Whittle in his scaling experiment. Fourth, we used all four possible combinations of test and pedestal polarity in our pedestal discrimination experiment, as illustrated in Figure 3. A+ tests were combined with both A+ and A– pedestals, and similarly for A– tests. Cole et al. (1990) and Gabree, Shepard, and Eskew (2018) also used this fourfold TvC approach, which provides the most general test of the model sketched in Figure 1.

Consistent with previous studies, our results reveal qualitative differences between A+ and A– visual processing. Furthermore, we found a strong relationship between suprathreshold perceptual scales and pedestal discrimination. Our model shows that contrast discrimination could be well predicted from the perceptual scale, with only one free parameter for each polarity.

Methods

Observers

The same five practiced observers served in both experiments. Two are authors of this paper; the others were not aware of the purpose of the experiments. All observers had normal scores on the Farnsworth–Munsell 100-Hue Test and the Hardy, Rand, and Rittler (HRR) Pseudoisochromatic Plates test. They all had normal or corrected-to-normal visual acuity. This study was approved by the Northeastern University Institutional Review Board. All procedures followed the tenets of the Declaration of Helsinki. Informed consent was provided by all observers.

Apparatus

Stimuli were presented on a Sony GDM-F520 CRT monitor (Tokyo, Japan), run at a frame rate of 85 Hz, driven by a Bits# stimulus processor (Cambridge Research Systems, Rochester, UK). The intensity nonlinearity of the display was corrected by a lookup table loaded into the Bits#. Calibrations were performed using a PR650 spectroradiometer (Photo Research, Chatsworth, CA). Experiments were controlled by a Mac Pro computer (Apple, Cupertino, CA), running the OS X El Capitan operating system (version 10.11.6). The experiment script was written in MATLAB R2016b (MathWorks, Natick, MA) using the Psychtoolbox (Brainard, 1997; Kleiner, Brainard, & Pelli, 2007).

Observers sat 129 cm in front of the monitor, with their dominant eye aligned to the center, and the other eye was patched. Non-emmetropic observers viewed the display through an ophthalmic trial lens. The distance between the dominant eye and trial lens was approximately 13 mm. All stimuli were scaled to account for the (very small) spectacle magnification caused by the trial lens.

Stimuli

The stimuli in Experiments 1 and 2 shared the same spatial layout (Figure 2) and temporal waveform (a 329 ms rectangular flash). A 0.2° fixation cross was constantly in the center of the screen. Four squares subtending 1.5° each surrounded the cross. The diagonal distance between the cross center and the closest corner of each square was 0.5°. The fixation cross always remained on screen. The background always remained mid-gray, with a luminance of 104 cd/m^2 ($x = 0.289$, $y = 0.315$).

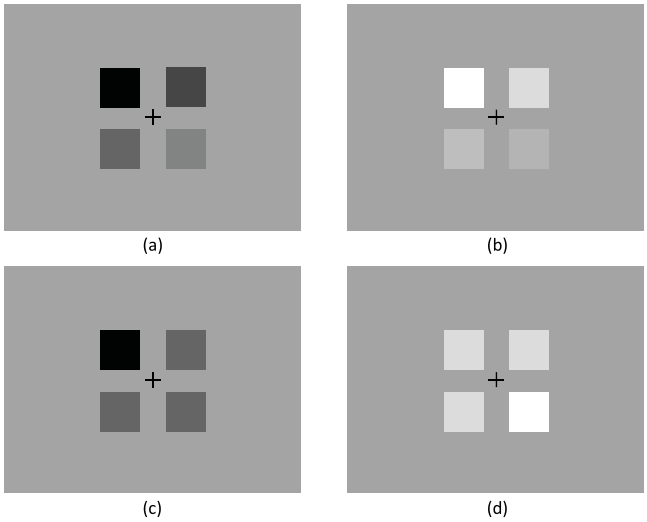

Figure 2. Example trials in both experiments. (a) A– MLDS; (b) A+ MLDS. In MLDS, observers compared the difference between the two stimuli in the top row and the difference between the two stimuli in the bottom row. (c) A– pedestal discrimination; (d) A+ pedestal discrimination. In discrimination, observers were instructed before the experiment run started to pay attention to the top pair (c) or bottom pair (d), randomly selected for each experimental run, and to choose the test, which appeared randomly on the left or the right. Also see Figure 3.

Contrast of a stimulus is defined by the luminance difference between the square and the background, divided by the background luminance ($\Delta I/I$, Weber contrast) (Westheimer, 1985). The maximum luminance contrasts we produced on the CRT monitor were ±0.9 in both polarities. The sign of contrast indicates the polarity, with positive and negative values for increments and decrements, respectively. We reanalyzed our results using Michelson contrast as well, as discussed in Appendix B.

Procedure

In a preliminary experiment, observers used the method of adjustment to set their threshold for both the A+ and A– polarities, separately, with all four squares having the same contrast. This procedure was repeated on two separate days, and the average was taken. Observers adapted to the mid-gray background for 60 seconds before every run in all experiments.

Experiment 1. Maximum likelihood difference scaling

Only one polarity (A– or A+) was tested in a given session (Figure 2). In each trial, the observer saw four squares at four different contrasts; this variation on

the MLDS procedure is referred to as the "method of quads" (see Knoblauch & Maloney, 2012). The observer was instructed to evaluate the difference between the two squares in the top pair and compare that to the difference between the two squares in the bottom pair. Four of the observers were told to choose the pair that was subjectively more similar. The fifth observer (TV) picked the pair that was more different. TV's results were very similar to the others who used the "similar" criterion. Observers initiated each presentation by pressing the space bar and made their selection using the top- or bottom-pointing arrows on the keyboard. A given stimulus pattern could be viewed as many times as the observer wanted before making a decision. Observers were instructed that they could fixate individual squares when necessary, but they should fixate in the center to make their final choice.

Eleven contrast values were linearly sampled from double the observer's threshold of the test condition to 0.9, which is the maximum contrast the monitor could produce. Each trial randomly presented four values from those 11 without repetition. This generated 330 trials in each session. The pairs of differences used did not overlap; the range of the top row contrasts did not include the contrast of either bottom square (for discussion, see Knoblauch & Maloney, 2012). Observers did two sessions for both conditions on separate days.

Experiment 2. Pedestal discrimination

At the start of an experimental run, the observer was instructed to attend to the top or bottom row (chosen randomly) of two squares for that run. In each trial (Figures 2c, 2d), all four of the squares had the same polarity (A+ or A–) as the pedestal stimulus. A test contrast was added to one of the two squares in the attended row, with the net result that three of the squares always had the same (pedestal) contrast, and the other square was the sum of the pedestal and test contrasts.

The task of the observer was to indicate whether the test was on the left or right side of the attended row. Observers controlled the stimulus presentation using the space bar as in Experiment 1, but only one presentation could occur in each trial.

Every run contained 100 trials. Within a run, the pedestal polarity (A+ or A–), the test polarity (A+ or A–), and the pedestal contrast stayed the same. Only the test contrast changed between trials, following an adaptive staircase procedure: The absolute value of the test contrast decreased by 0.1 log units after three correct responses and increased by the same amount after each error. This staircase aims to converge on 79% correct (Wetherill & Levitt, 1965). Two independent staircases were randomly interleaved in each run.

In a session, pedestal and test polarity were constant. Pedestal contrast changed in different runs but was constant within a run of 100 trials. Test contrast varied across trials. There were four polarity combinations in this experiment (Figure 3): A+ pedestal with A+ test, A+ pedestal with A– test, A– pedestal with A+ test, and A– pedestal with A– test. Observers repeated all runs at least three times on at least two separate days. Experiment 2 took each observer 10 to 12 hours in total.

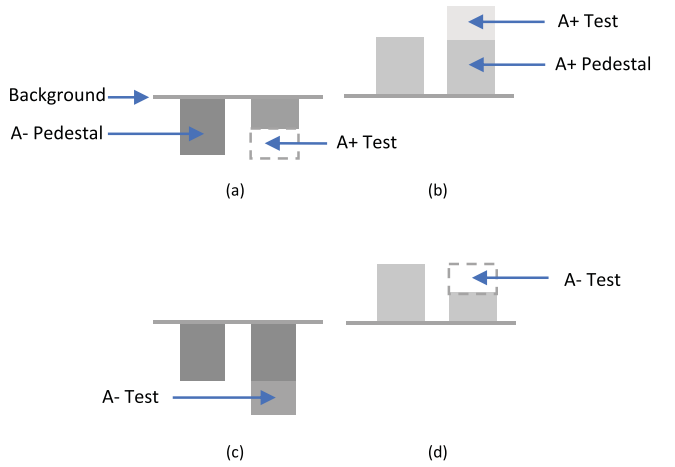

Figure 3. Four conditions of Experiment 2. The vertical extent of the bars represents luminance contrast. The horizontal line represents the luminance of the background, which was held constant throughout the experiment. Test locations were randomized in the experiment, but in this figure, they are all on the right. (a) A– pedestal, A+ test; (b) A+ pedestal, A+ test; (c) A– pedestal, A– test; (d) A+ pedestal, A– test.

Perceptual scale analysis

We used the MLDS model to analyze the data from Experiment 1 to construct a perceptual scale for each observer. The analysis was performed using MATLAB code (Harvey & Smithson, 2021). Following the model of Maloney and Yang (2003), we assumed that the response to each presentation at a given contrast was a sample from a normal distribution, with a mean that depended on the contrast level and a standard deviation σ that was constant across different contrast values (Figure 4). In one trial, there are four different contrast values: A, B, C, and D. Assume that AB make the top pair and CD make the bottom pair. Their corresponding mean perceptual scale values are ψ(A), ψ(B), ψ(C), and ψ(D). The procedure of choosing the more similar pair is summarized in Equation 1, as Maloney and Yang (2003) described it:

$$\Delta = [\psi(A) - \psi(B)] - [\psi(C) - \psi(D)] + \varepsilon \quad (1)$$

where Δ represents the perceptual comparison result in a given trial, and ε represents the total noise involved in the decision, based on a sample from a normal

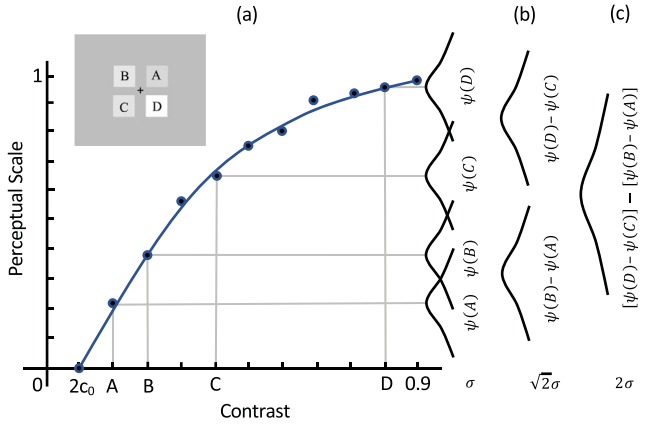

Figure 4. A schematic result of Experiment 1. (a) The horizontal axis is luminance contrast, and the vertical axis is the perceptual scale (normalized to be between 0 and 1). The 11 data points represent the estimated perceptual scale values of the sampled contrast values, and C_0 is the detection threshold. The curve is a modified Naka–Rushton equation (see text). The example trial (see text) is highlighted by the gray lines. A, B, C, and D are contrast values of four squares; ψ represents the means of the corresponding perceptual scale normal distributions; and σ is a constant noise shared by those distributions. (b) The first-stage comparison between the pairs of stimuli (with first-stage comparison noises $\sqrt{2}\sigma$). (c) The resulting decision variable distribution (Equation 1), with decision noise 2σ. These various sources of error are not capable of being estimated in a single application but are included here to illustrate the general ideas. Figure modified from figure 6 of Shooner and Mullen (2022).

distribution, with a mean of zero and a standard deviation of 2σ. If the perceptual difference within the AB pair is larger than that within the CD pair, then Δ will be larger than zero, on average; otherwise, Δ will be smaller than zero on average, and the observer is assumed to choose the stimulus pair based upon the sign of Δ. All trial results are then fit through an optimization procedure described in Maloney and Yang (2003). The procedure assigns all 11 contrast values each a corresponding perceptual scale value that maximizes the likelihood of the data collected. The perceptual scale values of the lowest and the highest contrast are set to 0 and 1 (the standard scale defined by Knoblauch & Maloney, 2012). The fixed noise σ is also estimated in this procedure. For each polarity, we pooled the data from two sessions together before MLDS analysis. We found that either analyzing this way or running the MLDS on data from two sessions separately and then averaging the MLDS results produced almost identical results.

The MLDS model returns perceptual scale values only at the tested contrasts. To make a continuous perceptual scale, we fit the A+ estimates with a modified Naka–Rushton (Michealis–Menton) equation (Naka & Rushton, 1966), as others have done (Knoblauch, Marsh-Armstrong, & Werner, 2020; Werner, Marsh-Armstrong, & Knoblauch, 2020) (Equation 2a). However, the A– scale values were clearly not simply a decelerating function of stimulus strength like the A+ values and could not be described by the same function. Therefore, in the case of A–, we fit a third-order polynomial instead (Equation 2b):

$$P_+ = \left[1 + \frac{m_+}{(C_m - 2C_{0+})}\right] \times \frac{(C_+ - 2C_{0+})}{(C_+ - 2C_{0+}) + m_+} \quad (2a)$$

$$P_- = b \times C_-^3 + d \times C_-^2 + e \times C_- + f \quad (2b)$$

Both equations were constrained to go through the first and the last data scale points (where contrast is at double the threshold and where it is at maximum), as we used the normalized perceptual scale in which the perceptual scale of smallest and largest contrasts are assigned to be 0 and 1. In the equations, P is perceptual magnitude, C is contrast (+ or –), C_m is the maximum contrast tested, C_0 is detection threshold, and m_+ is the constant estimated by fitting in Equation 2a. Appendix A provides further details.

Pedestal discrimination analysis

For each run, we fit a Weibull function to the accumulated frequency-of-seeing data, using a maximum-likelihood method (Watson, 1979), to extract a location and slope parameter. Threshold was taken to be the location parameter, which gives the contrast at 82% detection. Thresholds were averaged over at least three runs for each condition, with those runs being performed on at least two separate days.

Modeling and prediction

With a fixed background luminance, an observer's pedestal discrimination threshold depends on the pedestal contrast. As others have done, we assumed that this threshold is inversely proportional to the rate of change of perceptual scale curve at that pedestal contrast level (e.g., Legge & Foley, 1980; Shooner & Mullen, 2022). Therefore, at a particular contrast, if the slope of the perceptual scale curve is low, the discrimination threshold should be high, and conversely. The influence of perceptual noise in pedestal discrimination was also considered. Equation 3 is our prediction model:

$$C_t = k_{A_\pm} \times \sigma_{A_\pm} \times \frac{1}{\frac{d}{dc} p\left(C_{ped}\right)} \quad (3)$$

In Equation 3, C_{ped} is the pedestal contrast, C_t is the pedestal discrimination threshold (the contrast of the test), the denominator is the derivative of the perceptual

scale curve at contrast level C_{ped}, σ is the standard deviation of the noise (estimated by the MLDS model), and k is the only free parameter. Both k and σ are potentially different for different pedestal polarities (A+ and A–). Interpretation of the k parameter is addressed in the Discussion section. To evaluate the goodness of fit, we calculated the square of the correlation between the predicted and obtained mean thresholds across pedestal contrasts and the root-mean-square error (RMSE).

Results

Results from Experiment 1 are plotted in Figure 5. The observers' perceptual scale for A+ follows a decelerating curve, as is often reported for bipolar stimuli (e.g., Shooner & Mullen, 2022; Werner et al., 2020). In contrast, for A–, the scale is a reversed, inverted "S" shape. As the magnitude of the negative contrast increases from threshold, the scale values change rapidly, then more slowly, then more rapidly. For both A+ and A– perceptual scales, the steep region near the origin represents the crispening effect (Whittle, 1992), in which perceived magnitude changes rapidly with contrast. Crispening is observed in all observers' perceptual scales. but there are individual differences among observers in the magnitude of the crispening effect, with observers YS and JH showing the effect most clearly. Estimated values of σ for A+ are all higher than those for A– (Table 1), which suggests that there is greater noise in the perceptual representation of increments than decrements.

In Experiment 2, we investigated the pedestal discrimination threshold on different pedestal conditions and pedestal contrasts. The results are plotted in Figure 6. On A+ pedestals, the thresholds increased as the pedestal contrast increased. On A– pedestals, the thresholds first increased with the magnitude of pedestal contrast, but after reaching the peak (near the middle point between mid-gray and maximum decrement contrast), they decreased again.

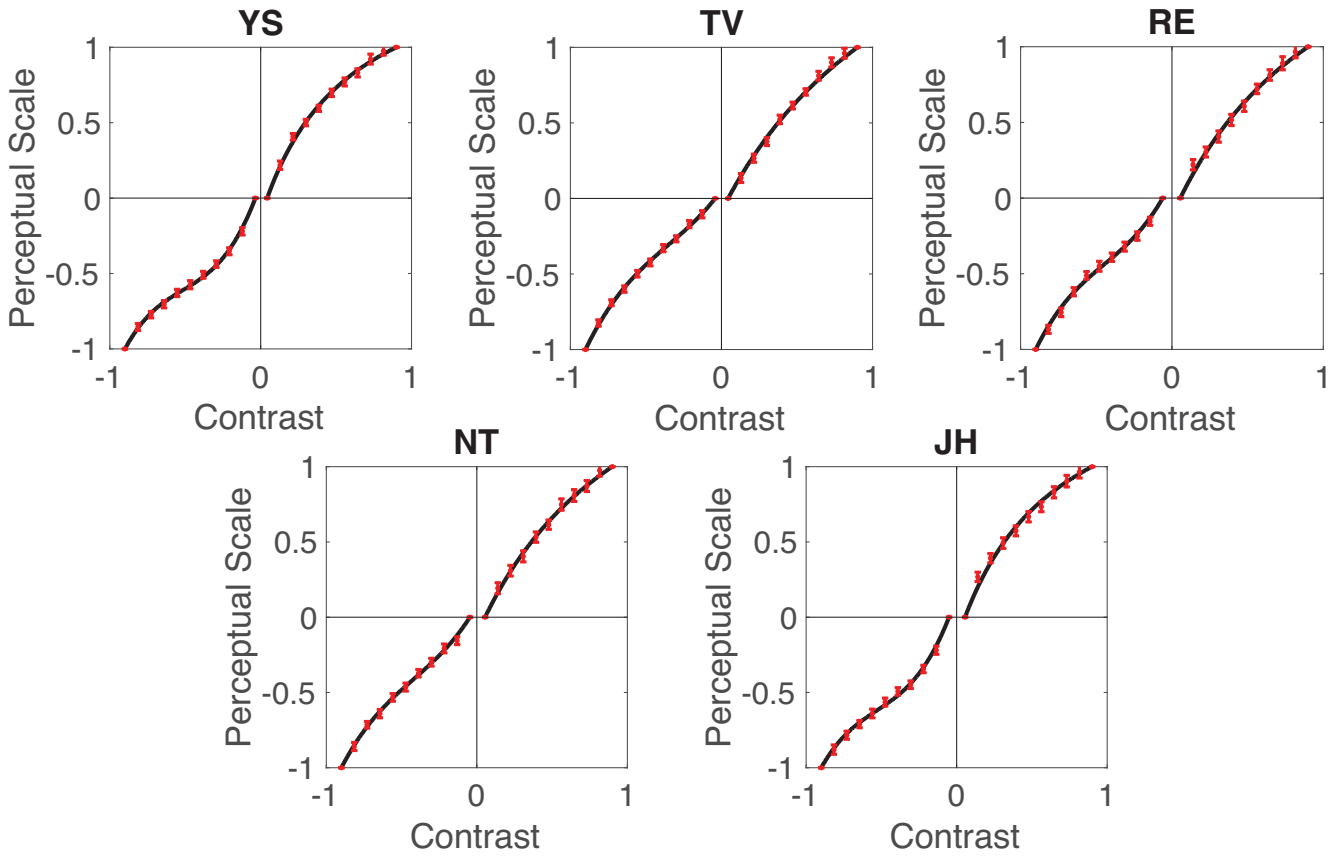

Figure 5. Perceptual scales estimated by MLDS for five observers. The origin represents the adaptation state. The horizontal axis is contrast, and the vertical axis is the perceptual scale. The red points are the discrete estimates of the MLDS model. Error bars are 95% bootstrap confidence intervals. Black curves are best fits of Equations 2a and 2b. A+ is plotted in the first quadrant, and A– is plotted in the third quadrant.

Condition	Observer				
	YS	TV	RE	NT	JH
A+ perceptual scale (Equation 2a)					
m_+	0.618	1.454	1.175	1.130	0.676
A+ prediction (Equation 3)					
k_{A_+}	0.514	0.527	0.576	0.409	0.315
σ_{A_+}	0.090	0.110	0.149	0.149	0.128
A– perceptual scale (Equation 2b)					
b	2.878	1.363	1.979	1.532	2.721
d	–4.470	–1.448	–2.656	–1.945	–4.340
e	2.910	1.371	2.025	1.703	2.968
f	–0.097	–0.055	–0.114	–0.074	–0.139
A– prediction (Equation 3)					
k_{A_-}	0.208	0.335	0.415	0.247	0.154
σ_{A_-}	0.087	0.079	0.117	0.098	0.112

Table 1. Parameters in equations

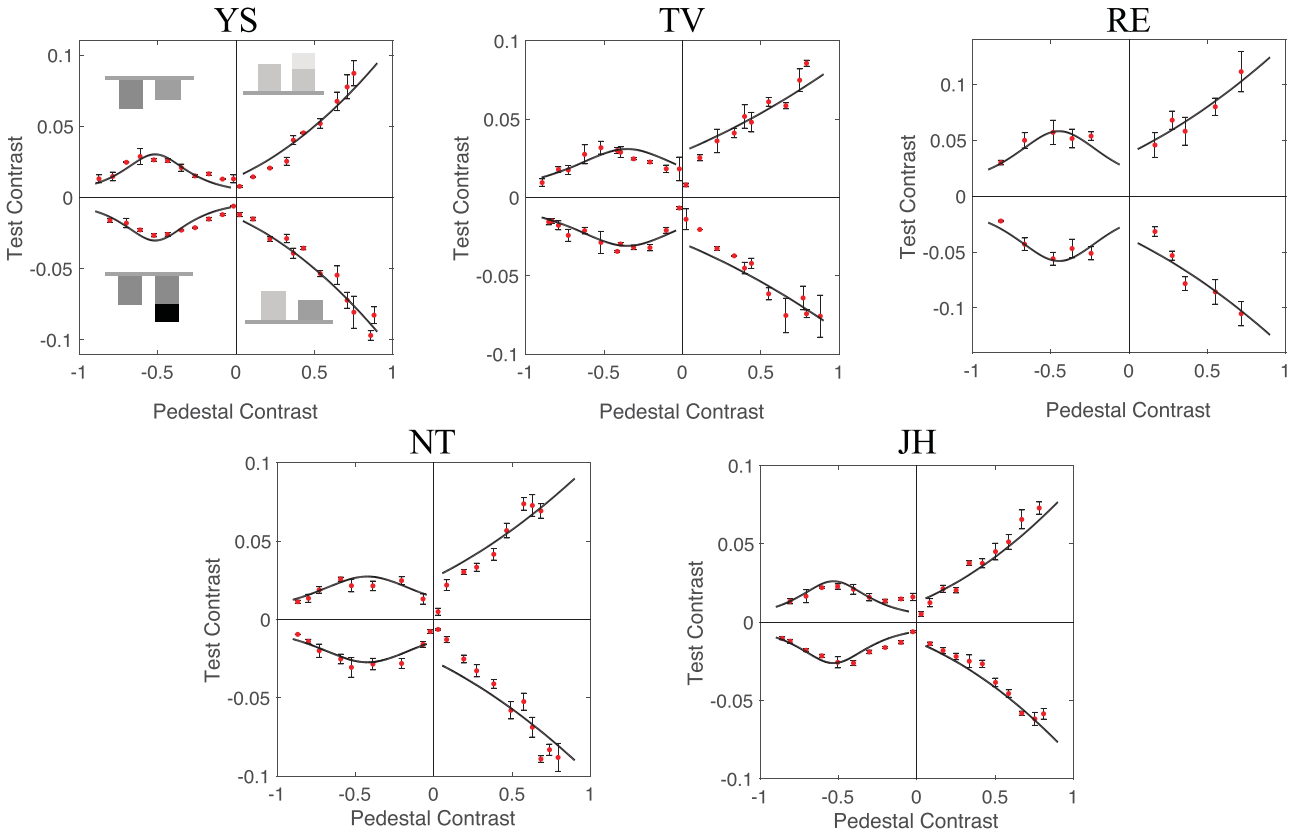

Figure 6. Pedestal discrimination thresholds. The origin represents the mid-gray, adapting field. Pedestal contrasts are plotted on the horizontal axis, and threshold test contrasts are plotted on the vertical axis. The positive halves of both axes represent increments, and the negative halves of both axes represent decrements. From the first quadrant to the fourth quadrant, the discrimination conditions are A+ test, A+ pedestal; A+ test, A– pedestal; A– test, A– pedestal; A– test, A+ pedestal (cf. Figure 3). Each data point is the mean of all the test thresholds on the given pedetal contrast; the error bars are standard errors based only on between-run variability. The continuous curves represent the prediction based on Equation 3.

	Observer				
Condition	YS	TV	RE	NT	JH
A+, R^2	0.94	0.85	0.86	0.84	0.92
A+, *RMSE*	0.006	0.007	0.009	0.009	0.005
A–, R^2	0.62	0.75	0.74	0.74	0.55
A–, *RMSE*	0.003	0.003	0.006	0.003	0.003

Table 2. Measures of goodness of fit to predicted thresholds

Our model predictions are plotted as curves over the discrimination results. Detailed parameters of the models are listed in Table 1. In all cases, the predictions (Equation 3) based on our perceptual scale model (A+: modified Naka–Rushton, Equation 2a; A–: third-order polynomial, Equation 2b) fit the data well. The estimated k values are all higher for A+ than A–. The goodness of fit (square of correlation and RMSE) of the predictions is summarized in Table 2. The fit is generally good for incremental contrasts, but is worse for decremental ones.

The cubic function was used as a reasonable first approximation to describe the perceptual scale for decrements. Although the fit to the perceptual scale is quite good, the derivative of the cubic function is a quadratic and therefore symmetric, and that required symmetry apparently leads to a worse fit to the pedestal discrimination thresholds in Figure 6. Further exploration of the true perceptual scale for decrements, ideally based on natural image statistics and physiological considerations, is worthy of future study but is beyond the scope of the current paper.

We also tried analyzing our data in Michelson contrast (details in Appendix B). We found that the prediction model provided a substantially better fit to the data when Weber contrast was used instead of Michelson contrast.

Discussion

Our study investigated suprathreshold perceptual scales and pedestal discrimination for incremental and decremental achromatic contrast. There are two major findings. First, both our experiments demonstrated again the perceptual asymmetry between A+ and A–. Second, and more importantly, we determined that the perceptual scale and contrast discrimination do not stand alone, as the contrast discrimination can be well predicted using the perceptual scale. Consistency between discrimination thresholds and suprathreshold appearance has been found in many cases (e.g., Aguilar, Wichmann, & Maertens, 2017; Devinck & Knoblauch, 2012; Shooner & Mullen, 2022; Whittle, 1992) but not all (e.g., Protonotarios, Johnston, & Griffin, 2016; Sato, Nagai, Kuriki, & Nakauchi, 2016).

In our results, for A+, the perceptual scale follows a compressive curve, and pedestal discrimination thresholds rise monotonically with pedestal contrast. For A–, the perceptual scale follows an inverted, reversed "S"-shaped curve, and discrimination thresholds follow a nonmonotonic curve as the model predicts. For both polarities, we observed a crispening effect near the detection thresholds, where the perceived magnitude changes rapidly with contrast.

Constant and noise

Our model consists of two parts. The first part, $k_{A_\pm} \times \sigma_{A_\pm}$, is perceptual noise multiplied by a constant, and the second part, $\frac{1}{\frac{d}{dc}p(c_{ped})}$, is the inverse of the derivative of the perceptual scale. The different perceptual scales themselves might result from contrast gain control mechanism differences in the ON and OFF pathways, as discussed below, and the derivatives in the second part of the model reflect those differences.

In the first part of our model, the constant $k_{A_\pm}$ is the only free parameter. A simple interpretation of it is that it is a constant that converts between two procedures: perceptual scale measurement and two-alternative forced-choice (2AFC) discrimination. According to signal detection theory, in a 2AFC task, to reach the correct rate of 82% used to define our thresholds, the distance between the internal representation of two stimuli should be $\sqrt{2} \times Z(0.82) \times \sigma = 1.29\sigma$ (Wickens, 2001), and that should be true for both A+ and A– because k represents a proportionality between procedures and does not have anything to do with light polarities. However, all of the k values we estimated are much smaller than 1.29, and differ for increments and decrements. For A+, the mean k value is 0.47, and that for A− is even lower, 0.27.

There might be two reasons for these low k values. First, MLDS is a suprathreshold difference scaling method. Though it is robust in generating the contrast response function, it is possible that the estimated noise level is not precise, as the scaling result is largely independent of the estimate of σ (Kingdom, 2016). In our case, the noise estimated by MLDS might be larger than the actual noise level for the 2AFC task. If the scaling noise is larger than discrimination noise, it would cause the k values to be smaller than predicted. Second, in our pedestal discrimination experiment, to make the stimulus pattern the same as that in the MLDS experiment, we kept all four squares as the stimulus. Though observers were told to only pay attention to two of those squares, the other two squares still provided extra information about the pedestal, which made the task easier. This extra information could cause discrimination thresholds to be smaller than predicted, leading to smaller estimated k values.

Although the two factors we suggest above might explain why the k values are smaller than 1.29, they do not explain why the k values for A+ are higher than those for A–. To explain this difference, we would have to postulate that MLDS overestimates σ to a larger degree for A– than for A+, an idea that is purely speculative. Thus, although our model provides a good empirical translation between MLDS and 2AFC pedestal discrimination, the interpretation of its parameters requires further exploration. Finally, as is always true when fitting a model to data, the fact that the model provides a good account of the data does not necessarily mean the model is correct; however, in this case, the ability of the MLDS model to predict the results of a completely separate experiment (2AFC discrimination) gives us confidence that the general outline of the model, at least, is correct.

ON and OFF pathways

The observed psychophysical asymmetries are likely to result from differences in physiology that begin early in vision. Incremental and decremental signals are processed separately by ON and OFF pathways starting at the very first synapse between photoreceptors and bipolar cells in the retina (Hartline, 1938; Nelson & Kolb, 2004; Schiller, 1992; Schiller, 2010; Werblin & Dowling, 1969). This separation can be found in the lateral geniculate nucleus (LGN) and is maintained until at least V1 (Harris & Parker, 1995; Jin et al., 2008). The two pathways have been shown to have functional differences. Studies have found significant OFF pathway advantages (e.g., contrast sensitivity and processing speed) over the ON pathway in the retina (Chichilnisky & Kalmar, 2002), LGN (Jiang, Purushothaman, & Casagrande, 2015a; Jiang, Purushothaman, & Casagrande, 2015b; Jiang, Yampolsky, Purushothaman, & Casagrande, 2015), and visual cortex (Kremkow et al., 2014; Xing, Yeh, & Shapley, 2010; Yeh, Xing, & Shapley, 2009). Our finding that pedestal discrimination thresholds for A– at high contrasts are lower than those for A+ at high contrasts suggests lower contrast gain control in OFF pathways, which is consistent with these studies.

The A+ perceptual scale curve saturates at high contrast. In contrast, the cubic function shape of the A– perceptual scale curve does not saturate but instead is closer to a flat function. Contrast gain control differences might help explain this shape difference (for S-cone discrimination asymmetry, see also the discussion in Gabree et al., 2018). Previous research has reported that ON pathway cells have larger receptive fields than OFF pathway cells (Archer, Alitto, & Usrey, 2021; Chichilnisky & Kalmar, 2002; Ravi, Ahn, Greschner, Chichilnisky, & Field, 2018). Ravi et al. (2018) proposed that larger receptive fields are consistent with shorter integration time. Archer et al. (2021) further proposed that neurons that have a shorter integration time should have more contrast gain control. Putting these together, we suggest that the larger receptive fields in the ON pathway cause more contrast gain control in the ON than in the OFF pathway. This gain control difference leads to larger compression in the A+ perceptual scale than the A– and thus to differences in discrimination performance.

Conclusions

The present results add to the extensive body of psychophysical differences between visual processing of increments and decrements. The perceptual scales for increments and decrements differ dramatically in shape, and those shapes predict forced-choice discrimination of contrasts for both polarities.

At least two questions remain. One is why previous studies—for example, Shooner and Mullen (2022), Knoblauch et al. (2020), and Bellot et al. (2016), who used visual patterns containing both A+ and A– in their MLDS experiment—found a decelerating perceptual scale like our A+ scale despite their stimuli containing both incremental and decremental contrasts. One might expect their results to be a mixture of the two polarity scales or even to be dominated by decrement perception, given the higher sensitivity to decrements. Instead, their MLDS scale and discrimination findings with gratings are like our increment results.

The major unresolved issue is this: Even if the differences between A+ and A– can be attributed to detection via ON and OFF pathways, *why* does our visual system produce such large, qualitative differences in increment and decrement vision? Statistical analysis has found that there are more negative than positive contrasts in natural images (Ratliff, Borghuis, Kao, Sterling, & Balasubramanian, 2010). More importantly, the physical nature of positive and negative contrasts is asymmetric. Given an adaptation state, negative contrasts are limited to the range between –1 and 0, but positive contrasts are 0 to positive infinity. It is possible that smaller receptive fields and less contrast gain control in OFF cells provide a better match to natural image statistics.

Keywords: MLDS, pedestal discrimination, ON–OFF, decrement, increment

Acknowledgments

The authors are grateful for the observing work of Nicholas Trent, Victoria Vance, and Jingyi He.

Supported by a grant from the National Science Foundation (BCS 2239356).

Commercial relationships: none.
Corresponding author: Rhea T. Eskew, Jr.
Email: r.eskew@northeastern.edu.
Address: Department of Psychology, Northeastern University, Boston, MA 02115, USA.

References

Aguilar, G., Wichmann, F. A., & Maertens, M. (2017). Comparing sensitivity estimates from MLDS and forced-choice methods in a slant-from-texture experiment. *Journal of Vision, 17*(1):37, 1–18, https://doi.org/10.1167/17.1.37.

Archer, D. R., Alitto, H. J., & Usrey, W. M. (2021). Stimulus contrast affects spatial integration in the lateral geniculate nucleus of macaque monkeys. *The Journal of Neuroscience, 41*(29), 6246–6256, https://doi.org/10.1523/JNEUROSCI.2946-20.2021.

Baird, J. C., & Noma, E. J. (1978). *Fundamentals of scaling and psychophysics*. New York: John Wiley & Sons.

Bellot, E., Coizet, V., Warnking, J., Knoblauch, K., Moro, E., & Dojat, M. (2016). Effects of aging on low luminance contrast processing in humans. *NeuroImage, 139*, 415–426, https://doi.org/10.1016/j.neuroimage.2016.06.051.

Brainard, D. H. (1997). The psychophysics toolbox. *Spatial Vision, 10*(4), 433–436.

Chichilnisky, E. J., & Kalmar, R. S. (2002). Functional asymmetries in ON and OFF ganglion cells of primate retina. *The Journal of Neuroscience, 22*(7), 2737–2747, https://doi.org/10.1523/JNEUROSCI.22-07-02737.2002.

Chichilnisky, E. J., & Wandell, B. A. (1996). Seeing gray through the ON and OFF pathways. *Visual Neuroscience, 13*(3), 591–596, https://doi.org/10.1017/S0952523800008270.

Cole, G. R., Stromeyer, C. F., 3rd, & Kronauer, R. E. (1990). Visual interactions with luminance and chromatic stimuli. *Journal of the Optical Society of America A, 7*(1), 128–140, https://doi.org/10.1364/josaa.7.000128.

Devinck, F., & Knoblauch, K. (2012). A common signal detection model accounts for both perception and discrimination of the watercolor effect. *Journal of Vision, 12*(3):19, 1–14, https://doi.org/10.1167/12.3.19.

Foley, J. M., & Legge, G. E. (1981). Contrast detection and near-threshold discrimination in human vision. *Vision Research, 21*(7), 1041–1053, https://doi.org/10.1016/0042-6989(81)90009-2.

Gabree, S. H., Shepard, T. G., & Eskew, R. T., Jr. (2018). Asymmetric high-contrast masking in S cone increment and decrement pathways. *Vision Research, 151*, 61–68, https://doi.org/10.1016/j.visres.2017.06.017.

Harris, J. M., & Parker, A. J. (1995). Independent neural mechanisms for bright and dark information in binocular stereopsis. *Nature, 374*(6525), 808–811, https://doi.org/10.1038/374808a0.

Hartline, H. K. (1938). The response of single optic nerve fibers of the vertebrate eye to illumination of the retina. *American Journal of Physiology–Legacy Content, 121*(2), 400–415.

Harvey, J. S., & Smithson, H. E. (2021). Low level visual features support robust material perception in the judgement of metallicity. *Scientific Reports, 11*(1), 16396, https://doi.org/10.1038/s41598-021-95416-6.

Jiang, Y., Purushothaman, G., & Casagrande, V. A. (2015a). A computational relationship between thalamic sensory neural responses and contrast perception. *Frontiers in Neural Circuits, 9*, 54, https://doi.org/10.3389/fncir.2015.00054.

Jiang, Y., Purushothaman, G., & Casagrande, V. A. (2015b). The functional asymmetry of ON and OFF channels in the perception of contrast. *Journal of Neurophysiology, 114*(5), 2816–2829, https://doi.org/10.1152/jn.00560.2015.

Jiang, Y., Yampolsky, D., Purushothaman, G., & Casagrande, V. A. (2015). Perceptual decision related activity in the lateral geniculate nucleus. *Journal of Neurophysiology, 114*(1), 717–735, https://doi.org/10.1152/jn.00068.2015.

Jin, J. Z., Weng, C., Yeh, C. I., Gordon, J. A., Ruthazer, E. S., Stryker, M. P., . . . Alonso, J. M. (2008). On and off domains of geniculate afferents in cat primary visual cortex. *Nature Neuroscience, 11*(1), 88–94, https://doi.org/10.1038/nn2029.

Kane, D., & Bertalmio, M. (2019). A reevaluation of Whittle (1986, 1992) reveals the link between detection thresholds, discrimination thresholds, and brightness perception. *Journal of Vision, 19*(1):16, 1–13, https://doi.org/10.1167/19.1.16.

Kaneko, T. (1964). A reconsideration of the Cobb-Judd lightness function. *Acta Chromatica, 1*, 103.

Kingdom, F., & Moulden, B. (1991). A model for contrast discrimination with incremental and decremental test patches. *Vision Research, 31*(5), 851–858, https://doi.org/10.1016/0042-6989(91)90152-u.

Kingdom, F. A. A. (2016). Fixed versus variable internal noise in contrast transduction: The significance

of Whittle's data. *Vision Research, 128*, 1–5, https://doi.org/10.1016/j.visres.2016.09.004.

Kleiner, M., Brainard, D., & Pelli, D. (2007). What's new in Psychtoolbox-3? *Perception, 36*, 14.

Knoblauch, K., & Maloney, L. T. (2012). *Modeling psychophysical data in R*. London: Springer Nature.

Knoblauch, K., Marsh-Armstrong, B., & Werner, J. S. (2020). Suprathreshold contrast response in normal and anomalous trichromats. *Journal of the Optical Society of America A, 37*(4), A133–A144, https://doi.org/10.1364/JOSAA.380088.

Kremkow, J., Jin, J., Komban, S. J., Wang, Y., Lashgari, R., Li, X., . . . Alonso, J. M. (2014). Neuronal nonlinearity explains greater visual spatial resolution for darks than lights. *Proceedings of the National Academy of Sciences, USA, 111*(8), 3170–3175, https://doi.org/10.1073/pnas.1310442111.

Kwon, M., Legge, G. E., Fang, F., Cheong, A. M., & He, S. (2009). Adaptive changes in visual cortex following prolonged contrast reduction. *Journal of Vision, 9*(2):20, 1–16, https://doi.org/10.1167/9.2.20.

Laming, D. R. J. (1973). *Mathematical psychology*. London: Academic Press.

Legge, G. E., & Foley, J. M. (1980). Contrast masking in human vision. *Journal of the Optical Society of America, 70*(12), 1458–1471, https://doi.org/10.1364/josa.70.001458.

Legge, G. E., & Kersten, D. (1983). Light and dark bars; contrast discrimination. *Vision Research, 23*(5), 473–483, https://doi.org/10.1016/0042-6989(83)90122-0.

Maloney, L. T., & Yang, J. N. (2003). Maximum likelihood difference scaling. *Journal of Vision, 3*(8):5, 573–585, https://doi.org/10.1167/3.8.5.

Nachmias, J., & Kocher, E. C. (1970). Visual detection and discrimination of luminance increments. *Journal of the Optical Society of America, 60*(3), 382–389, https://doi.org/10.1364/josa.60.000382.

Nachmias, J., & Sansbury, R. V. (1974). Letter: Grating contrast: Discrimination may be better than detection. *Vision Research, 14*(10), 1039–1042, https://doi.org/10.1016/0042-6989(74)90175-8.

Naka, K. I., & Rushton, W. A. (1966). S-potentials from colour units in the retina of fish (Cyprinidae). *Journal of Physiology, 185*(3), 536–555, https://doi.org/10.1113/jphysiol.1966.sp008001.

Nelson, R., & Kolb, H. (2004). ON and OFF pathways in the vertebrate retina and visual system. *The Visual Neurosciences, 1*, 260–278.

Protonotarios, E. D., Johnston, A., & Griffin, L. D. (2016). Difference magnitude is not measured by discrimination steps for order of point patterns. *Journal of Vision, 16*(9):2, 1–17, https://doi.org/10.1167/16.9.2.

Ratliff, C. P., Borghuis, B. G., Kao, Y. H., Sterling, P., & Balasubramanian, V. (2010). Retina is structured to process an excess of darkness in natural scenes. *Proceedings of the National Academy of Sciences, USA, 107*(40), 17368–17373, https://doi.org/10.1073/pnas.1005846107.

Ravi, S., Ahn, D., Greschner, M., Chichilnisky, E. J., & Field, G. D. (2018). Pathway-Specific asymmetries between ON and OFF visual signals. *The Journal of Neuroscience, 38*(45), 9728–9740, https://doi.org/10.1523/JNEUROSCI.2008-18.2018.

Rudd, M. E., & Zemach, I. K. (2004). Quantitative properties of achromatic color induction: An edge integration analysis. *Vision Research, 44*(10), 971–981, https://doi.org/10.1016/j.visres.2003.12.004.

Rudd, M. E., & Zemach, I. K. (2005). The highest luminance anchoring rule in achromatic color perception: Some counterexamples and an alternative theory. *Journal of Vision, 5*(11):, 983–1003, https://doi.org/10.1167/5.11.5.

Sato, T., Nagai, T., Kuriki, I., & Nakauchi, S. (2016). Dissociation of equilibrium points for color-discrimination and color-appearance mechanisms in incomplete chromatic adaptation. *Journal of the Optical Society of America A, 33*(3), A150–163, https://doi.org/10.1364/JOSAA.33.00A150.

Schiller, P. H. (1992). The ON and OFF channels of the visual system. *Trends in Neurosciences, 15*(3), 86–92, https://doi.org/10.1016/0166-2236(92)90017-3.

Schiller, P. H. (2010). Parallel information processing channels created in the retina. *Proceedings of the National Academy of Sciences, USA, 107*(40), 17087–17094, https://doi.org/10.1073/pnas.1011782107.

Shooner, C., & Mullen, K. T. (2022). Linking perceived to physical contrast: Comparing results from discrimination and difference-scaling experiments. *Journal of Vision, 22*(1):13, 1–16, https://doi.org/10.1167/jov.22.1.13.

Solomon, J. A. (2009). The history of dipper functions. *Attention, Perception, and Psychophysics, 71*(3), 435–443, https://doi.org/10.3758/APP.71.3.435.

Takasaki, H. (1967). Chromatic changes induced by changes in chromaticity of background of constant lightness. *Journal of the Optical Society of America, 57*(1), 93–96, https://doi.org/10.1364/josa.57.000093.

Watson, A. B. (1979). Probability summation over time. *Vision Research, 19*(5), 515–522, https://doi.org/10.1016/0042-6989(79)90136-6.

Werblin, F. S., & Dowling, J. E. (1969). Organization of the retina of the mudpuppy, *Necturus maculosus*. II. Intracellular recording. *Journal of Neurophysiology, 32*(3), 339–355, https://doi.org/10.1152/jn.1969.32.3.339.

Werner, J. S., Marsh-Armstrong, B., & Knoblauch, K. (2020). Adaptive changes in color vision from long-term filter usage in anomalous but not normal trichromacy. *Current Biology, 30*(15), 3011–3015.e4, https://doi.org/10.1016/j.cub.2020.05.054.

Westheimer, G. (1985). The oscilloscopic view: Retinal illuminance and contrast of point and line targets. *Vision Research, 25*(8), 1097–1103, https://doi.org/10.1016/0042-6989(85)90098-7.

Westheimer, G. (2007). The ON-OFF dichotomy in visual processing: From receptors to perception. *Progress in Retinal and Eye Research, 26*(6), 636–648, https://doi.org/10.1016/j.preteyeres.2007.07.003.

Wetherill, G. B., & Levitt, H. (1965). Sequential estimation of points on a psychometric function. *British Journal of Mathematical and Statistical Psychology, 18*, 1–10, https://doi.org/10.1111/j.2044-8317.1965.tb00689.x.

Whittle, P. (1986). Increments and decrements: Luminance discrimination. *Vision Research, 26*(10), 1677–1691, https://doi.org/10.1016/0042-6989(86)90055-6.

Whittle, P. (1992). Brightness, discriminability and the "crispening effect". *Vision Research, 32*(8), 1493–1507, https://doi.org/10.1016/0042-6989(92)90205-w.

Wickens, T. D. (2001). *Elementary signal detection theory*. Oxford, UK: Oxford University Press.

Xing, D., Yeh, C. I., & Shapley, R. M. (2010). Generation of black-dominant responses in V1 cortex. *The Journal of Neuroscience, 30*(40), 13504–13512, https://doi.org/10.1523/JNEUROSCI.2473-10.2010.

Yeh, C. I., Xing, D., & Shapley, R. M. (2009). "Black" responses dominate macaque primary visual cortex v1. *The Journal of Neuroscience, 29*(38), 11753–11760, https://doi.org/10.1523/JNEUROSCI.1991-09.2009.

Appendix A: Equations for MLDS

The equations fit to the MLDS (Equation 2a and 2b) were constrained to go through the lowest and highest data points.

Derivation of Equation 2a

Equation 2a is a modified Naka–Rushton equation. The equation is used to fit a curve to 11 discrete A+ perceptual scale values. We started from the following Naka–Rushton equation:

$$P = P_{max} \times \frac{C^n}{C^n + m^n} \quad \text{(A1)}$$

where P is perceptual scale magnitude, P_{max} is the maximum perceptual scale amplitude, c is contrast, m is a semi-saturation constant, and n is the exponent of the function.

The contrast values we used in MLDS experiments were between double the detection thresholds ($2C_0$) and maximum contrasts we produced on the monitor (C_m). Also, we used the standard scale for MLDS, which sets the perceptual scale values of lowest and highest contrasts to be 0 and 1. We thus modified Equation A1 to go through those two fixed data points, which are ($2C_0$, 0) and (C_m, 1). Additionally, we picked $n = 1$. To go through ($2C_0$, 0), this gives us Equation A2:

$$P_+ = P_{max} \times \frac{C - 2C_0}{C - 2C_0 + m} \quad \text{(A2)}$$

We leave parameter m as a coefficient to be estimated. Then, we use (C_m, 1) to find P_{max} using parameter m. Equation A2 now becomes

$$1 = P_{max} \times \frac{C_m - 2C_0}{C_m - 2C_0 + m} \quad \text{(A3)}$$

So, we find $P_{max} = \frac{C_m - 2C_0 + m}{C_m - 2C_0}$. Substituting this value into Equation A2 gives Equation 2a.

Constraints for Equation 2b

In Equation 2b, free parameters b, d, e, and f were fit to the data, with the following constraints:

$$b \times {C_m}^3 + d \times {C_m}^2 + e \times C_m + f = 1 \quad \text{(A4)}$$

$$b \times 8C_{0-}^3 + d \times 4C_{0-}^2 + e \times 2C_{0-} + f = 0 \quad \text{(A5)}$$

Notice that when we are fitting the perceptual scale for A–, the fitting procedure treated both contrast and the perceptual scale as positive numbers. However, in later figures, to differentiate A+ and A–, we used negative signs for A– contrasts and perceptual scales.

Appendix B: Weber contrast and Michelson contrast analysis

Here, we reanalyze our MLDS and discrimination data in terms of Michelson contrast, following the approach of Legge and Kersten (1983). In general, Michelson contrast is defined as (max – min)/(max + min), where max and min refer to the maximum and minimum luminance values of a stimulus.

As shown in Figure 2, all stimuli we used are squares. In the pedestal discrimination experiment, there are pedestal squares and test squares. The luminance of a pedestal square is L_{ps}, the luminance of a test square is L_{ts}, and the background luminance is L_b. The difference

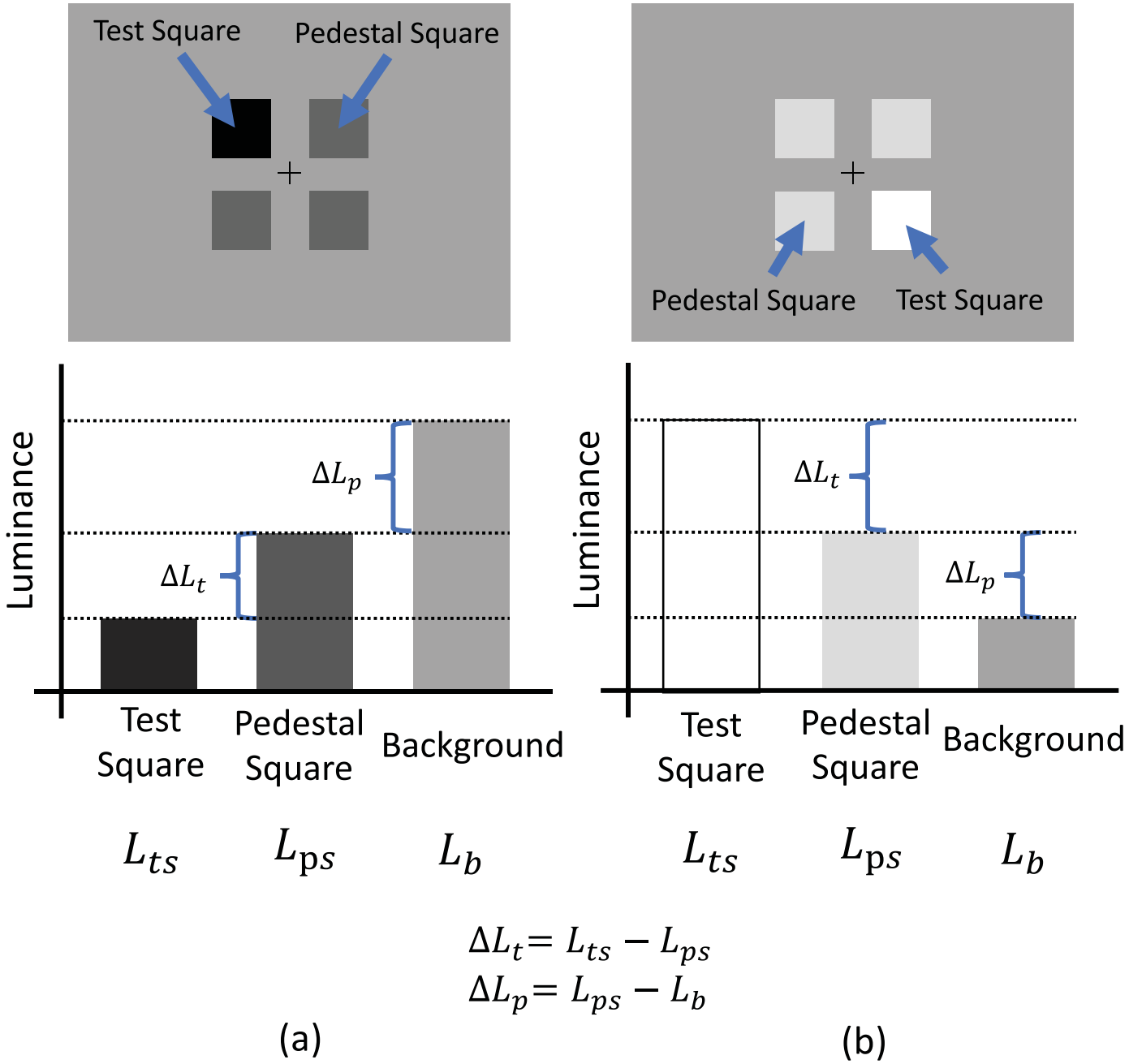

Figure B1. Definition of luminance of squares and differences between them, illustrated using the discrimination experiment example from Figure 2. The first row shows discrimination trials. (a) The A– pedestal, A– test; the test square is on the left in the top pair. (b) The A+ pedestal, A+ test; the test square is on the right in the bottom pair. The second row shows the luminance of the test square L_{ts}, pedestal square L_{ps}, and background L_b in those trials. The third row shows how test luminance ΔL_t and pedestal luminance ΔL_p are calculated. Notice that ΔL_t and ΔL_p are signed quantities.

of two luminance values is defined using ΔL. ΔL_p is the luminance difference between the pedestal square and the background. ΔL_t is the luminance difference between the test square and the pedestal square. These luminance differences are signed quantities. For example, in Figure B1, ΔL_t and ΔL_p in column (a) are both negative, whereas in column (b) they are both positive. Avoiding negative luminance values requires that $L_b \geq \Delta L_p + \Delta L_t$ for both positive and negative values of ΔL_p and ΔL_t. In our analysis, we modeled the relationship between pedestal contrast C_p and test contrast C_t. They are calculated differently depending on whether Weber contrast or Michelson contrast is used.

The Weber contrast (C_p) of a pedestal square against our fixed luminance background is calculated using luminance difference between the pedestal square and the background divided by the background luminance:

$$C_{p,Weber} = \frac{\Delta L_p + L_b - L_b}{L_b} = \frac{\Delta L_p}{L_b} \quad \text{(B1)}$$

The Michelson contrast ($C_{p,Michelson}$) of the same pedestal square is calculated using the luminance difference divided by the sum of luminance:

$$C_{p,Michelson} = \frac{\Delta L_p + L_b - L_b}{\Delta L_p + L_b + L_b} = \frac{\Delta L_p}{\Delta L_p + 2L_b} \quad \text{(B2)}$$

The test contrast, which is the contrast difference between the pedestal square contrast and test square contrast, is simple in Weber contrast due to the common denominator for the two terms:

$$C_{t,Weber} = \frac{\Delta L_t + \Delta L_p}{L_b} - \frac{\Delta L_p}{L_b} = \frac{\Delta L_t}{L_b} \quad \text{(B3)}$$

The corresponding Michelson contrast expression is more complex due to the different denominators:

$$\begin{aligned} C_{t,\,Michelson} &= \frac{\Delta L_t + \Delta L_p + L_b - L_b}{\Delta L_t + \Delta L_p + L_b + L_b} - \frac{\Delta L_p + L_b - L_b}{\Delta L_p + L_b + L_b} \\ &= \frac{\Delta L_t + \Delta L_p}{\Delta L_t + \Delta L_p + 2L_b} - \frac{\Delta L_p}{\Delta L_p + 2L_b} \\ &= \frac{2L_b \Delta L_t}{(2L_b + \Delta L_p)(2L_b + \Delta L_p + \Delta L_t)} \end{aligned} \quad \text{(B4)}$$

Notice that in all our contrast calculations above, signs (polarities) have been considered in the equations. With these definitions, Michelson contrast can be positive or negative.

Increment and decrement ranges of Weber contrast are between 0 and ±0.9, which is symmetric. However, in Michelson contrast, the increment range is between 0 and 0.31, while the decrement range is between 0 and –0.82. The increment range is largely compressed.

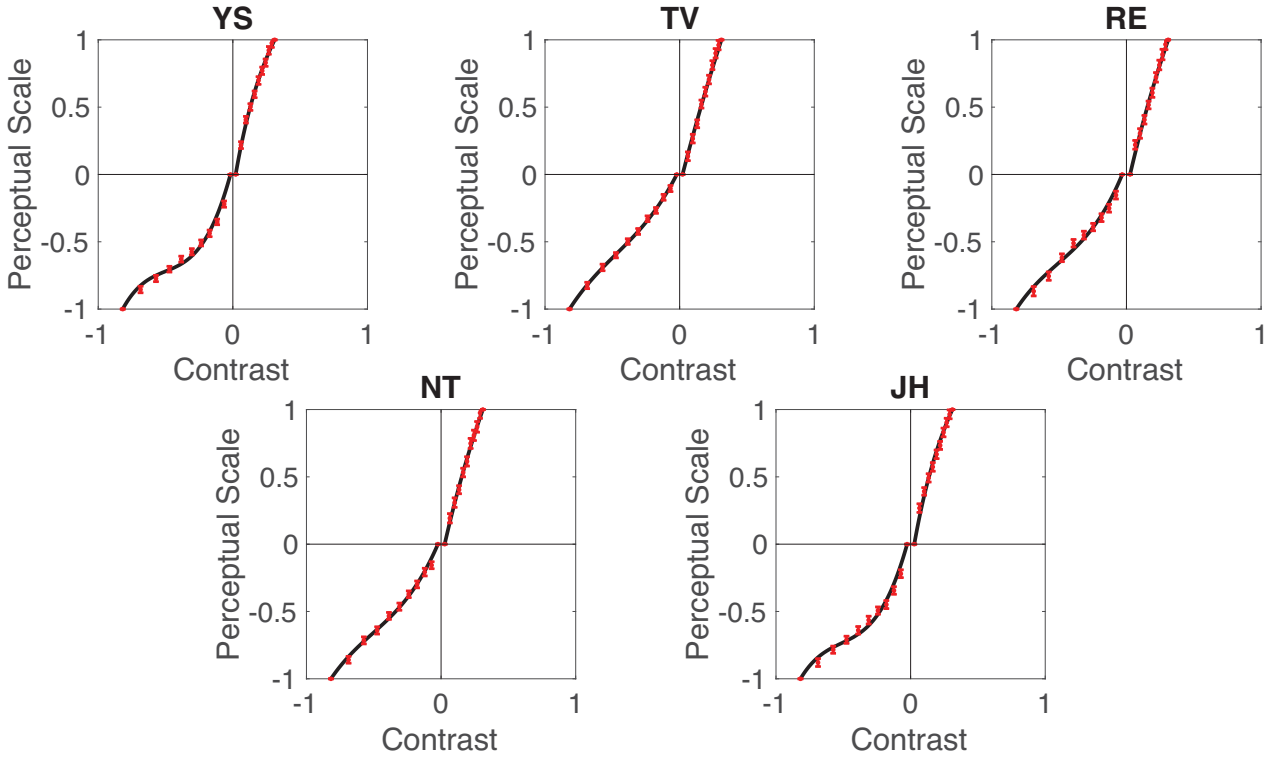

Figure B2. Figure 5 replotted in terms of Michelson contrast. The red points are MLDS model estimation. Error bars are 95% bootstrap confidence intervals. Black curves are best fits of Equations 2a and 2b. A+ is plotted in the first quadrant, and A– is plotted in the third quadrant.

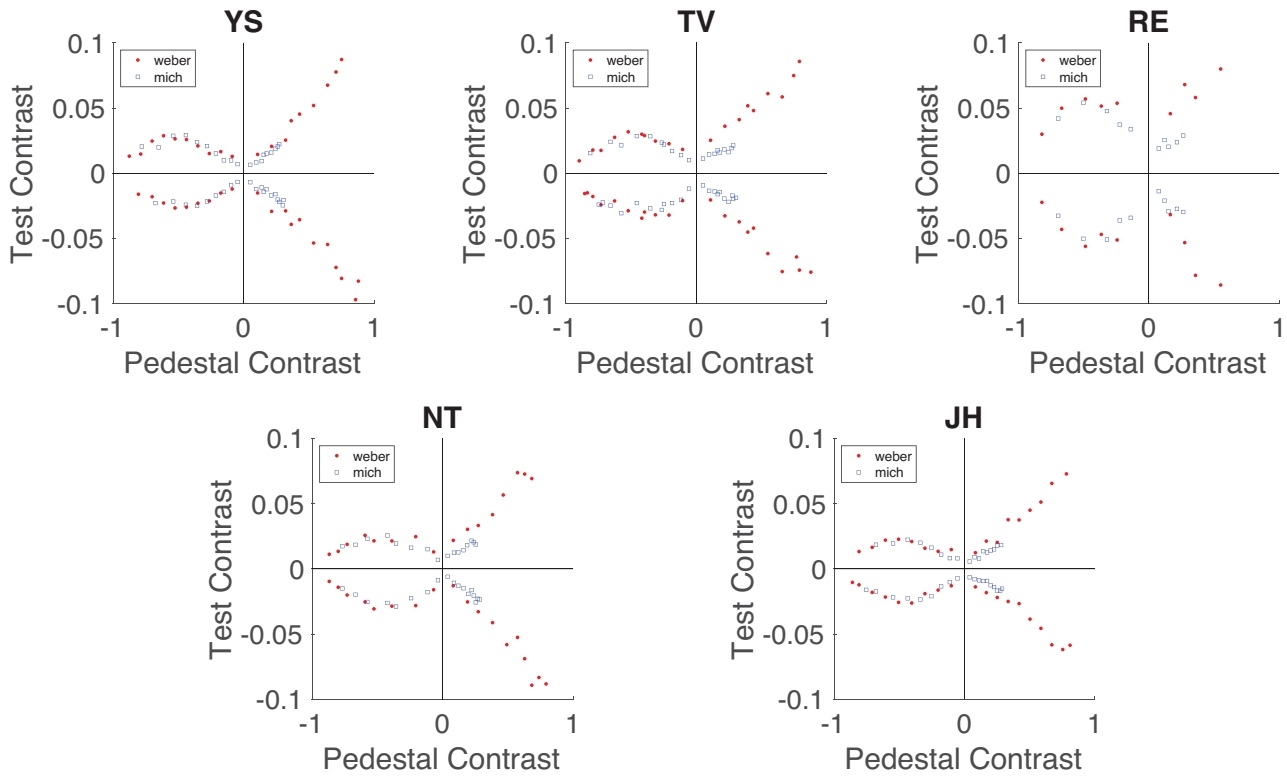

Figure B3. Pedestal discrimination results plotted in Weber contrast and Michelson contrast. Red filled circles are Weber contrast, blue open circles are Michelson contrast. As in Figure 6, the horizontal axis represents pedestal contrast, and the vertical axis represents test contrast.

Figure B2 shows the MLDS results plotted and fit in Michelson contrast. The curve fits are still generally good. The A– perceptual scale is still in a reversed, inverted "S" shape. However, the A+ perceptual scale is not as saturated as it is when Weber contrast is used (Figure 5).

We plotted our pedestal discrimination results in Weber contrast and Michelson contrast together (Figure B3). In terms of Michelson contrast, discrimination thresholds on A+ pedestals still increase monotonically as pedestal contrast increases. The discrimination thresholds on A– pedestals still first increase as pedestal contrast increases, then decrease as pedestal contrast gets higher. Due to our limited Michelson contrast range (A+, 0 to 0.31; A–, –0.82 to 0), we can only directly compare discrimination threshold on the A+ and A– pedestals when the pedestal contrasts are low ($<\pm 0.31$). Similar to what Legge and Kersten (1983) found, when Michelson pedestal contrast is low, the test contrast on A+ and A– pedestals are less asymmetric; our results extend to higher A– contrasts than theirs do, however, and discrimination threshold are clearly decreasing at the higher contrast values, even using Michelson contrast. Using the Michelson contrast MLDS results shown in Figure B2, we used our model to predict Michelson contrast pedestal discrimination thresholds (Figure B4). Our model prediction follows the data points; however, the fit is not as good as that in Weber contrast (Figure 6).

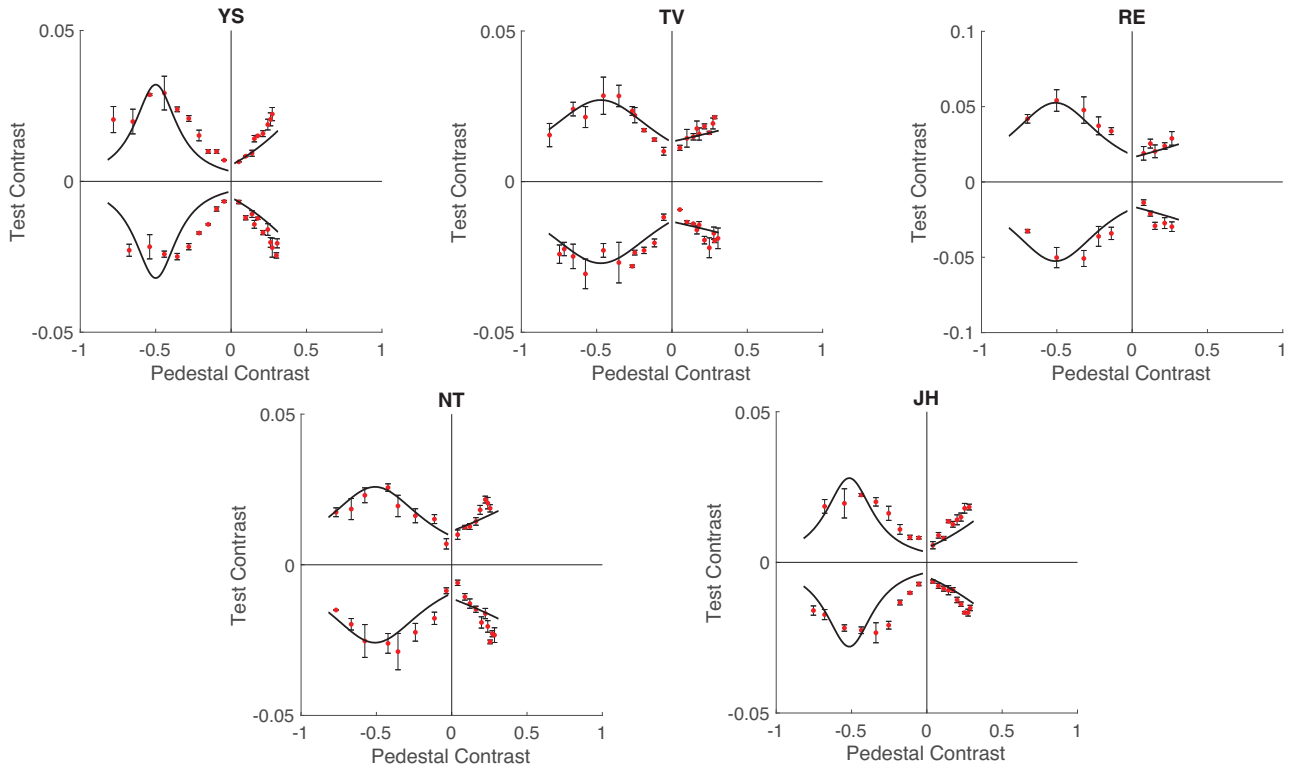

Figure B4. Pedestal discrimination results and model predictions based upon Michelson contrast. Red filled circles are pedestal discrimination results (error bars are standard errors). Black curves are the model predictions, using MLDS results in Michelson contrast. As Figure 6, the horizontal axis represents pedestal contrast, and the vertical axis represents test contrast.